

Better understanding on impact of microclimate information on building energy modelling performance for urban resilience

Lei Xu^a, Shanshan Tong^a, Wenhui He^a, Wei Zhu^a, Shuojun Mei^a, Kai Cao^b, Chao Yuan^{a,*}

^a Department of Architecture, National University of Singapore, Singapore

^b School of Geographic Sciences, East China Normal University, China



ARTICLE INFO

Keywords:

Building energy modelling
Weather data
EnergyPlus
Anthropogenic heat, Urban resilience

ABSTRACT

Building Energy Modelling (BEM) plays a significant role in projecting future building energy demands and predicting urban climate resilience in the context of climate change and urbanization. Accurate weather data are important components in BEM. In this study, we investigate how the BEM performance is affected by weather datasets, including 1) the typical meteorological year (TMY) data, 2) data measured at the suburban ground, and 3) three microclimate datasets, i.e., data measured at a high-rise rooftop near the site, data measured at the near-ground open space close to the site, and developed microclimate data within the urban canopy layer at the site. The new microclimate data are developed by integrating near-ground measured data and microclimate modeling results using a practical GIS model. Compared with the actual energy usage, the predictions of BEM using the developed microclimate data show the least mean bias error of 6%, while the error is 12% when TMY data are used. We further utilize this method to develop microclimate datasets and predict residential energy consumptions under the short-term coronavirus pandemic and long-term climate change scenarios. The findings provide scientific support for the decision-making in future energy planning to improve urban climate resilience.

1. Introduction

1.1. Background

Globally, the building sector consumes approximately 30% of the total energy consumed by end-users (Wang et al., 2018) and induces massive greenhouse gas (GHG) emissions (Congedo et al., 2021). In 2019, the final energy use in the building sector grew to 128 EJ, and CO₂ emissions from buildings reached an all-time high level of 28% global CO₂ emissions (International Energy Agency, 2020). Key drivers of this record-breaking building energy consumption in 2019 were the increased demands for space cooling and extreme heatwaves in many regions when a strong El-Nino phenomenon elevated global temperatures (World Meteorological Organization, 2019). In Singapore, over 50% of electricity was consumed in buildings (Energy Market Authority, 2015), and the annual growth rate of the final energy consumption was 6.1% between 1990 and 2017 (Sheng, 2021). Urbanization and climate change might further increase the energy demand in an unsustainable manner. To create a sustainable built environment, the Singapore government established a goal to reduce 35% energy use intensities by 2030 from 2005 levels (Duarte et al., 2018). To meet this

goal, it is crucial to better understand how urban microclimates affect building energy consumption (Ciancio et al., 2018) and provide accurate energy projections for sustainable urban planning and development.

In 2020, the outbreak of the coronavirus disease (COVID 19) pandemic changed building energy consumption profiles substantially, due to shifted activities and energy uses from industrial and commercial sectors to the residential. Although the global energy demand in 2020 declined by 4% according to the International Energy Agency (International Energy Agency, 2021), the residential electricity demand was increased during the lockdown period, e.g., by 6–8% in the United States (Aberget al., 2020), 14% in Australia (Farrow, 2020) and 22% in Singapore (Energy Market Authority, 2021), compared with the same period in 2019 or the pre-COVID period. Moreover, the spatial and temporal heterogeneities of impacts on energy demands were complicated due to the dynamics of pandemics and energy mitigation measures (Jiang et al., 2021).

Therefore, both short-term and long-term building energy demands have been facing numerous uncertainties in the situations of COVID pandemics and continuing climate change. Projections of future building energy demand become unprecedented challenging. It is thus crucial to develop accurate models for the prediction of future building energy

* Corresponding author.

E-mail address: akiyuan@nus.edu.sg (C. Yuan).

demand, which plays a major role in urban climate resilience and sustainable development.

1.2. Literature review

Building energy consumption in the urban context is highly related to sustainable urban development (Li et al., 2016; Madlener & Sunak, 2011; Yamaguchi et al., 2007). On one hand, building energy consumption directly affects the anthropogenic heat (AH) emission, which is one of the main causes of the Urban Heat Island (UHI) effect (Li et al., 2019; Mirzaei, 2015; Yuan et al., 2020). On the other hand, elevated ambient air temperatures in urban areas increase the energy demand for space cooling in sub/tropical cities (Founda & Santamouris, 2017; Jamei et al., 2020; Pokhrel et al., 2019). Therefore, thoughtful climate-sensitive urban planning is crucial to improve the energy sustainability and climate resilience of cities (Jabareen, 2013; Molyneaux et al., 2012; Sharifi & Yamagata, 2016). To support the above, it is necessary to investigate and predict the building energy performance in urban areas to provide insights for stakeholders on urban energy planning and building energy retrofits at scale (Hong et al., 2020).

Building energy performance prediction models have been established at multiple temporal and spatial scales (Li et al., 2017; Mohammadi & Bilec, 2020) and can be mainly categorized into two types, i.e., statistical-based models and physics-based models. Statistical-based models were developed based on historical building energy consumption data and weather data (Zhao & Magoulès, 2012). The development of statistical-based models usually consists of four steps: data collection, data preprocessing, model training, and model testing. With the development of computer science, statistical-based models took advantage of machine learning algorithms, e.g., support vector machine (Dong et al., 2005), artificial neural network (Xu et al., 2019), decision tree (Tso & Yau, 2007), and XGboost (Mo et al., 2019), to conduct building energy consumption prediction. These models have been applied at different temporal scales, e.g., one day ahead (Luo et al., 2019), one week ahead (Mocanu et al., 2016), and one month ahead (Catalina et al., 2008), as well as at multiple spatial scales, e.g., at the building scale (Robinson et al., 2017), city scale (Kohler et al., 2016) and national scale (Auffhammer et al., 2017). However, statistical-based models are restricted to the availability of historical energy consumption data (Li et al., 2019). The modelling performance would deteriorate if the available data were limited. Moreover, it could be more difficult to predict the building energy consumption under future scenarios with uncertainty, such as the ongoing COVID pandemics and future climate change.

Unlike statistical-based models, physics-based models simulate building energy consumption based on heat transfer principles (Li et al., 2019) and require multiple inputs, i.e., outdoor weather parameters, building geometries, materials, operation schedules, power consumptions of electrical appliances, and occupants' behavior (Yang et al., 2016). With physics-based models, it is possible to investigate the impacts of an individual or several parameters on building energy modelling performance. Among the input parameters, weather data are one of the fundamental inputs in building energy simulation. The common practice in Building Energy Modelling (BEM) is to use the Typical Meteorological Year (TMY) data, which is generated based on long-term historical weather observations (Yang et al., 2012). However, TMY data might not well represent the local microclimate conditions affected by surrounding morphology and human activities, especially in high-density urban areas (Liu et al., 2017). Consequently, an increasing number of studies adopted the in-situ observed or simulated weather data for BEM in urban areas. The in-situ observed weather data were mostly obtained from nearby meteorological stations (Santamouris et al., 2001; Watkins et al., 2002) or field measurements (Chan, 2011). However, such in-situ weather data were often collected at a certain location and point-based, and thus it neglects the spatial variations of urban microclimate, e.g., air temperature in the high-density neighborhood.

Instead of using TMY data or observed urban temperatures, a few studies developed urban microclimate datasets for BEM, using either empirical or numerical models. However, both empirical and numerical models have the limitation to prepare the weather data for BEM. For example, empirical models were developed (Jusuf et al., 2009) to predict the microclimate temperatures in Singapore based on the rural temperature and a series of urban morphology variables, such as percent pavement, height to building area ratio, wall surface area, green plot ratio, and sky view factor. The impacts of urban microclimate on building energy consumption were thus predicted and analyzed (Ignatius et al., 2016; Liu et al., 2017). However, such empirical models were often site-specific and required long-term observed weather data at multiple points for model development. Some researchers proposed generating the localized weather data for BEM based on parametric interpretations of urban areas using non-computational fluid dynamics (CFD) tools, such as urban weather generators (Bueno et al., 2013; Palme et al., 2017) and localized actual meteorological year file creators (Bianchi & Smith, 2019). Such tools are practical, but they have low resolution and require calibration to be applied at various sites. To achieve high-resolution microclimate data, some researchers proposed coupling BEM and CFD programs, such as Fluent and SOLENE (Bouyer et al., 2011), OpenFOAM (Miller et al., 2018) and ENVI-met (Gobakis et al., 2017; Yang et al., 2012; Zhang & Gao, 2021). These high-resolution microclimate modelling results could be used as weather data in BEM, but CFD simulations are time-consuming, especially at the urban scale. Moreover, these models rarely considered the impact of AH from air conditioning (AC) systems on ambient air temperature in high-density urban areas, which is a common source of AH emission in summer seasons or tropical climates (Yuan et al., 2020). Therefore, cooling energy demands in buildings tend to be underestimated.

1.3. Research objectives and structure

Based on the above literature review, this study aims to develop a new practical methodology to provide microclimate data that is accurate enough for BEM, so that BEM performance can be improved. The novelty of this study can be summarized as follows: 1) a new framework is developed and implemented to provide a representative microclimate dataset for BEM; 2) a significant improvement on BEM performance is achieved using the weather dataset from the developed framework; 3) residential energy demands under the short-term coronavirus pandemic and long-term climate change scenarios are estimated and anticipated. In particular, the sensitivity of BEM performance on five different weather datasets is analyzed. The impacts of weather datasets on the predicted building energy performance are evaluated in comparison with the actual energy consumption data, which are provided by Energy Market Authority in Singapore (Energy Market Authority, 2015). Afterward, the best-performing weather dataset is used to estimate and anticipate building energy consumptions under two scenarios, i.e., COVID pandemic and future climate change, for planning better urban resilient environments.

The research structure is organized as follows. The BEM study area and target buildings are chosen and described in Section 2. In Section 3, energy model parameter settings using EnergyPlus are presented, e.g., building geometries, construction materials, household electric appliances, etc. In Section 4, we apply five weather datasets at BEM of the target residential buildings. The datasets include 1) TMY data, 2) data measured at the suburban ground, and 3) three microclimate datasets, i.e., data measured at a high-rise rooftop near the site, data measured at the near-ground open space close to the site and developed microclimate data within the urban canopy layer at the site. In Section 5, the monthly and hourly building energy consumption predictions using the above five weather datasets are compared with actual measured energy consumption data. In Section 6, the developed framework is used to provide microclimate datasets for BEM and predict the total and peak residential building energy demands under the short-term (COVID pandemic) and

long-term (climate change) scenarios, as the implementation on urban resilience planning. The main conclusions of this research and future study are presented in [Section 7](#).

2. Study area and target buildings

A typical high-density neighborhood, consisting of seven public housing residential buildings at Everton Park in Singapore, was selected in this study. These seven buildings are 12-story-high facing North or South, as shown in [Fig. 1](#). We categorized them into two groups based on their locations, namely the surrounding buildings (Buildings 1–6) and the central building (Building 7). Because ambient temperatures could be higher near the central building than those near the surrounding buildings. The gross floor areas are 9,552 m² and 10,048 m² and the average window-to-wall ratios are 0.31 and 0.41 for the individual surrounding buildings and the central building, respectively.

For the surrounding buildings, the bottom floor was designed for commercial uses (e.g., retailers and restaurants) and the upper eleven floors were for residence. Each residential floor has six 3-room flats and three 5-room flats, as shown in [Fig. 2\(a\)](#) for the floor plan. For the central building, the lower two floors were designed for commercial uses and the upper ten floors for residence. Each residential floor has two types of 3-room flats, as shown in [Fig. 2\(b\)](#), and each type has six flats.

The number of occupied flats ([Housing & Development Board, 2021](#)) and AC ownership in each building are listed in [Table 1](#). It is worth noticing that not all the residential flats are occupied or equipped with AC systems. Therefore, AC ownership rates were estimated based on site investigation.

3. Residential energy simulation

Energy consumption in each building was modelled using the EnergyPlus program ([Crawley et al., 2001](#)), as it is one of the most widely used physics-based BEM programs ([Crawley et al., 2001; Fumo, Mago & Luck, 2010; Li et al., 2019](#)). In this study, only the energy consumption in residential flats was modelled, and the commercial energy use was not included. The settings of BEM are described as follows.

3.1. Building geometry and thermal zones

Simplified multi-story building models were built up using the multiplier function in EnergyPlus ([U.S. Department of Energy, 2021](#)), to represent similar floors and flats. For the surrounding six buildings (Building 1–6), a 10-times multiplier was applied to represent the typical floors from the 2nd to 11th, while the top floor (12th floor) was modelled separately due to its roof's solar exposure. On each floor of surrounding buildings, two multipliers were applied to represent the 5-room flats (colored in white) and the central 3-room flats (colored in

light blue) respectively, while the 3-room flats at both ends (colored in dark blue) were modelled separately due to their distinctive solar exposure, as illustrated in [Fig. 3\(b\)](#). For the central building (Building 7) with a different design, a 9-times multiplier was applied to represent the typical floors from the 3rd to 11th, with the top floor being modelled separately. On each floor of the central building, two multipliers were used to represent the two types of 3-room flats (3R-a and 3R-b, colored in white and light blue respectively), while the 3-room flats at both ends (3R-a, colored in dark blue) were modelled separately, as illustrated in [Fig. 3\(c\)](#).

In each residential flat, only bedrooms were included in the modelling and merged into one thermal zone, and other rooms (e.g., living room, kitchen/dining room, and bathrooms) were considered as non-thermal zones since residents rarely use AC over there. Therefore, the number of the thermal zones in the EnergyPlus model equals the number of residential flats.

3.2. Building construction materials

The detailed building materials used in EnergyPlus models, and their U-values (representing thermal transmittance) are listed in [Table 2](#), according to the common construction materials used in the public housings in Singapore ([Building & Construction Authority, 2001](#)).

3.3. Schedules of electrical appliances and occupancy

According to the data given by Singapore National Climate Change Committee ([National Climate Change Committee, 2011](#)) and a previous study ([Liu et al., 2017](#)), the operation schedule and power consumptions of typical household appliances shown in [Table 3](#) are adopted in this study. Residents' activities were assumed according to ([Chua & Chou, 2010](#)) and listed in [Table 4](#).

3.4. AC settings

The energy demand of an AC system was estimated using an ideal cooling load model ([Martin et al., 2017](#)). A typical coefficient of performance (COP) of 3.0 was adopted based on previous studies on the residential energy performance in Singapore ([Bruegisauer et al., 2014; Chua & Chou, 2010](#)). Moreover, the temperature setpoint was set to be 25°C during nighttime sleeping hours (23:30–06:00), according to the suggestion by National Environment Agency in Singapore ([National Environment Agency, 2012](#)).

3.5. Natural ventilation rate

Natural ventilation strongly affects the indoor air temperature when AC is off ([Tong et al., 2019](#)) and the amount of accumulated heat to be

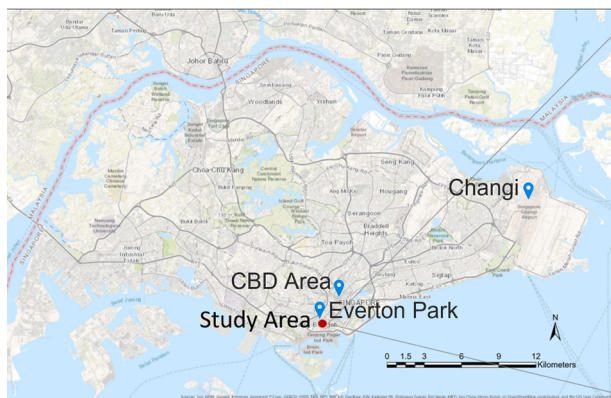


Fig. 1. Studied residential buildings at Everton Park in Singapore, a typical high-density neighborhood near the Central Business District.



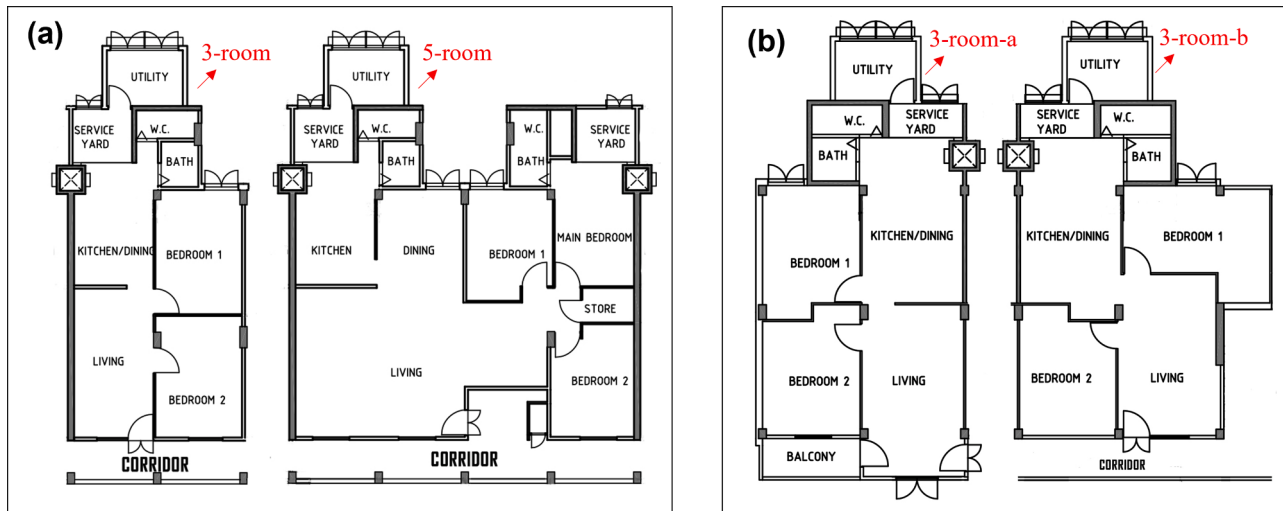


Fig. 2. Typical floor plans for (a) 3-room and 5-room flats in the surrounding buildings (Buildings 1–6), and (b) two types of 3-room flats in the central building (Building 7). Source: [Housing & Development Board, 2021](#).

Table 1
Characteristics of the target buildings.

	Building						
	1	2	3	4	5	6	7
No. of occupied 3-room flats	62	60	62	60	60	62	120
No. of occupied 5-room flats	33	34	34	34	34	33	0
AC ownership rate	100%	83%	88%	97%	97%	86%	91%

Note: AC ownership rate is defined as the number of outdoor AC condensers divided by the total number of occupied flats of a residential building.

removed when AC is on (Tong et al., 2021). In this study, windows of thermal zones were assumed open from 6:00 to 23:00, while those of non-thermal zones were open for 24 hours on sunny days and closed on rainy days. When windows were open, the indoor air change per hour (ACH) was estimated using Eq. (1) (Balasco et al., 2010):

$$ACH = \frac{0.65 \times U \times A_{win} \times 3600}{V_{room}} \quad (1)$$

where A_{win} is the area of window openings, in m^2 ; V_{room} is the volume of ventilated spaces, in m^3 ; U is the indoor wind speed, in m/s , and assumed to be 0.6 m/s according to the Singapore Green Mark criteria for a comfortable naturally ventilated environment (Building and Construction Authority, 2016). Therefore, the ACH was estimated to be 53

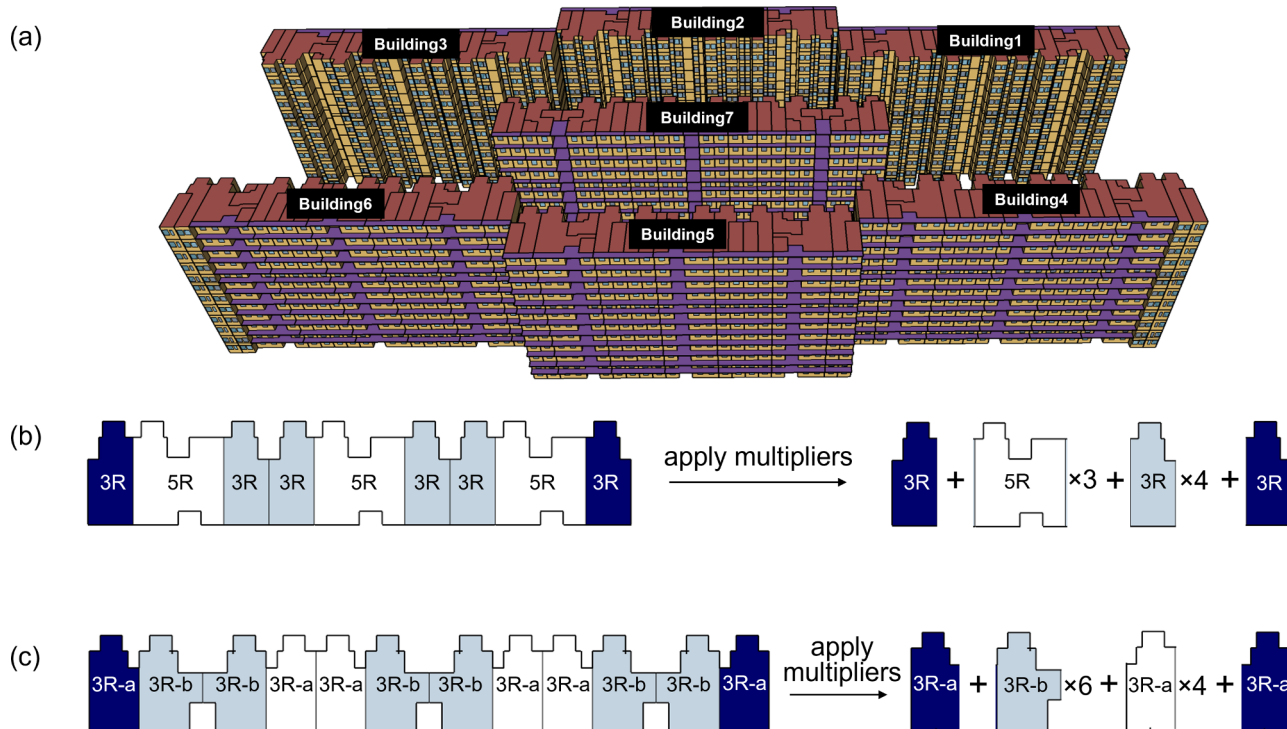


Fig. 3. Modelling configurations: (a) 3-dimensional view of target buildings, application of multipliers to (b) the surrounding buildings with 3-room (3R) and 5-room (5R) flats, and to (c) the central building with two types of 3-room flats (3R-a and 3R-b). Flats at both ends are colored in dark blue and modelled separately.

Table 2
Construction materials of modelled buildings.

Building component	Material	U-value (W/m ² K)
Window	6-mm clear glass	5.8
Interior wall	100-mm lightweight concrete	5.3
Exterior wall	150-mm heavyweight concrete + 75-mm Polyethylene + 5-mm cement plaster (from outside to inside)	0.31
Roof	30-mm ferrocement + 22-mm air space + 150-mm heavyweight concrete + 5-mm cement plaster (from outside to inside)	0.15
Floor	150-mm heavyweight concrete	13
Ceiling	150-mm heavyweight concrete	13

Table 3
Details of household electrical appliances in Singapore.

Household equipment	Power consumption (W)	Zone	Operation period (24 h)
Fan	39	Living room	08:00–18:30, 20:00–22:00
Lighting	40	Bedroom, kitchen, living room	06:00–07:00, 17:30–23:30
Refrigerator	106	Kitchen	00:00–24:00
Television	176	Living room	08:00–20:00
Computer	115	Living room	20:00–23:00
Kettle	2525	Kitchen	06:54–07:04
Electric iron	328	Kitchen	22:00–22:50
Washing machine	84	Bathroom	08:00–08:40
Rice cooker	724	Kitchen	06:30–07:00, 18:50–19:20

Table 4
Details of residents' activities.

Activity level (W)	Sleeping	Sitting
	72	108
Zone	Master bedroom	Common bedroom
People per zone	2	1
Schedule (24 h)	23:30–6:00	23:30–6:00
	08:00–20:00	20:30–23:00

for the naturally ventilated space in this study.

3.6. Infiltration rate

An infiltration rate of 0.5 was used for the air-conditioned space according to a recent local study (Liu et al., 2017).

3.7. Shading

Both corridor shading and inter-building shading were considered in EnergyPlus models since shading significantly affects the cooling energy consumption (Ascione et al., 2020).

More than the above settings, the EnergyPlus model assumed that all the thermal zones were occupied and air-conditioned, which was inconsistent with our onsite investigation. Therefore, the simulated energy consumption was adjusted using Eq. (2), to obtain the final total energy consumption in each building (E_{total} , kWh):

$$E_{total} = (E_{light} + E_{AC} \times AC_ownership + E_{plug_load}) \times \frac{N_{occ_flats}}{N_{flats}} \quad (2)$$

where E_{light} , E_{AC} , and E_{plug_load} are the energy consumptions by lighting, AC and other plug loads, respectively, in kWh; N_{occ_flats} and N_{flats} are the number of occupied flats and total flats in individual residential buildings, respectively; and $AC_ownership$ is the AC ownership rate in individual residential buildings.

4. Weather data

In this study, the impacts of weather datasets on the BEM performance of target buildings in June 2015 were analyzed. The month of June was selected as it is the hottest throughout the year in Singapore (Martin et al., 2017). The analyzed five weather datasets include 1) the TMY data, 2) data measured at an airport meteorological station, and 3) three microclimate datasets, i.e., data measured at a high-rise rooftop near the site, data measured at the near-ground open space close to the site and developed microclimate data within the urban canopy layer at the site, as summarized in Table 5 and Fig. 7. The distances between the target buildings and the Changi, Newton, and Marina Barrage stations are about 18.7 km, 3.7 km and 3.4 km, respectively. The first four weather datasets are introduced in Section 4.1, and the last type is described in Section 4.2.

4.1. TMY and measured weather data

The commonly used TMY weather data were obtained from the weather database provided in EnergyPlus, which adopts the weather data collected in June 1993 near Changi Airport in Singapore. The three measured weather datasets were collected in June 2015 at three meteorological stations, namely Changi, Newton, and Marina Barrage to represent a wide variety of urban morphologies and local climatic conditions (Kolokotroni & Giridharan, 2008). The measured hourly weather data include the ambient dry-bulb air temperature, relative humidity, wind speed, and solar radiations (i.e., global horizontal radiation, direct normal radiation, and diffuse horizontal radiation). According to (Kolokotroni et al., 2012), the site-specific temperature, relative humidity, wind speed, and solar irradiation data were processed using the EnergyPlus weather converter tool (U.S. Department of Energy, 2016) to generate the weather files for building energy simulation.

4.2. Developed microclimate data

In this study, the developed microclimate data was obtained in two steps: 1) selection of the closest near-ground weather station to the study area, to make the modelling more efficient and accurate and avoid testing weather datasets one by one; 2) further integration of the measured weather data at the selected station and the microclimate modelling results in the street canyon. Specifically, the measured weather data from the nearest near-ground meteorological station (at Marina Barrage) were combined with the modelled local temperature increments due to AH using a semi-empirical model developed in our previous study (Mei & Yuan, 2021; Yuan et al., 2020). It was found in a numerical simulation study that urban temperatures due to AH might increase by up to 2.3°C at 23:00–00:00 on a monthly average in Singapore (Yuan et al., 2020).

To obtain the hourly air temperature increment (ΔT_c) near the target buildings, AH from AC systems was firstly estimated based on simulated cooling loads in EnergyPlus using weather data at Marina Barrage. Secondly, ΔT_c was estimated using the analytical model developed in Geographic Information System (GIS) for local climate (Yuan et al., 2020) considering the impact of surrounding urban morphology and AH emission during the same hour, as given in Eq. (3):

$$\Delta T_c = \frac{1}{D_c} \frac{Q_{A_site}}{U_{ref} \cdot (1 - \lambda_p)} \left(1 - 0.12 \left(\frac{2}{\lambda_f} \right)^{0.5} \right) \quad (3)$$

where D_c is the heat capacity of the air at 17.183 J/Km³; Q_{A_site} is the

Table 5

Summary of weather datasets applied at BEM.

Dataset	Location	Time period	Measurement height (m)	Type	Description
A	Changi (TMY)	June 1993	7	Historical	Obtained from the original TMY file recorded at the suburban near-ground airport.
B	Changi (suburban ground)	June 2015	7	Measured	Collected from a meteorological station at the suburban near-ground airport.
I	Newton (urban rooftop)	June 2015	115	Measured	Collected from a meteorological station at a high-rise building rooftop near the site.
II	Marina Barrage (urban ground)	June 2015	15	Measured	Collected from a meteorological station at an near-ground open space close to the site.
III	Everton Park (street canyons)	June 2015	/	Developed	Developed by integrating the measured weather data at Marina Barrage and modelled temperature increments due to AH emission from AC within the street canyon at the site.

onsite AH emission rate of AC systems, in W; U_{ref} is the ambient wind velocity measured at $2H$ (H is the building height) above the roof level, in m/s; λ_f and λ_p are the site coverage ratio and frontal area density at 0.6 and 0.26, respectively. According to (Mei & Yuan, 2021), the temperature increment for tall buildings needs to be modified by a buoyancy coefficient (C_b), which represents the enhancement of exchange rate due to the buoyancy effect and is given by Eq. (4).

$$C_b = \frac{UE_t}{UE_n} \quad (4)$$

where UE_t and UE_n are the exchange rates under the non-isothermal and the isothermal conditions, respectively. The impact of buoyancy effect on urban ventilation has been widely investigated and quantified in existing numerical studies (Chen et al., 2020; Cheng et al., 2009; Li et al., 2010; Li et al., 2012; Mei et al., 2016; Xie et al., 2006), as illustrated in Fig. 4. C_b is linearly correlated to a buoyancy parameter B (i.e., $C_b = 0.1B + 1.05$) based on previous studies, and B is estimated by Eq. (5):

$$B = \frac{ga\Delta T \times H}{U_{ref}^2 [1 + (H/L)^2]} \quad (5)$$

where $ga\Delta T$ is the buoyancy term generated by exterior heated walls; H is the building height, in m; and L is the street width, in m. Therefore, the air temperature increment formula is given by Eq. (6).

$$\Delta T_c = \frac{1}{0.1B + 1.05} \frac{1}{D_c} \frac{Q_{A_site}}{U_{ref}(1 - \lambda_p)} \left(1 - 0.12 \left(\frac{2}{\lambda_f} \right)^{0.5} \right) \quad (6)$$

It should be noted that the modelled air temperature increment (ΔT_c) is a spatially averaged value for the studied area. As illustrated in Fig. 5, all the four facades of the central building are exposed to AH emission,

while only one facade of each surrounding building is exposed, due to the locations of AC condensers. In this case, the temperature increment (ΔT_c) calculated using Eq. (6) is only suitable for the central building. For each surrounding building, a modified temperature increment ($\Delta T'_c$) was used, and it is weighted by the ratio of façade areas exposed to AH emission, as given by Eq. (7).

$$\Delta T'_c = \Delta T_c \times \frac{FA_{affected}}{FA_{all}} \quad (7)$$

where $FA_{affected}$ is the façade area of a surrounding building exposed to AH emission, in m^2 ; FA_{all} is the total façade areas of a surrounding building, in m^2 . The ratio of exposed façade area ($FA_{affected}/FA_{all}$) was estimated to be 0.66 for the surrounding buildings based on field survey and building information.

Therefore, hourly temperature increments around all seven buildings in June 2015 were modelled based on the simulated cooling loads using weather data at Marina Barrage. Boxplots of estimated hourly temperature increments during nighttime (i.e., AC operation hours) in June 2015 are given in Fig. 6. (a) and (b) for the central building and surrounding buildings, respectively. It is observed that the medians of the hourly air temperature increments ranged from 1.16°C to 1.27°C around the central building, and from 0.77°C to 0.84°C around the surrounding buildings. A new microclimate dataset was thus developed by adding the predicted hourly local temperature increment of ΔT_c (or $\Delta T'_c$) to the hourly air temperature measured at Marina Barrage for the BEM of the central building (or surrounding buildings).

A summary of five weather datasets used in the EnergyPlus models is presented in Table 5 and Fig. 7. It is worth noting that the single-point measurement datasets at Changi, Newton and Marina Barrage were observed at the elevation heights of 7 m, 115 m, and 15 m, respectively.

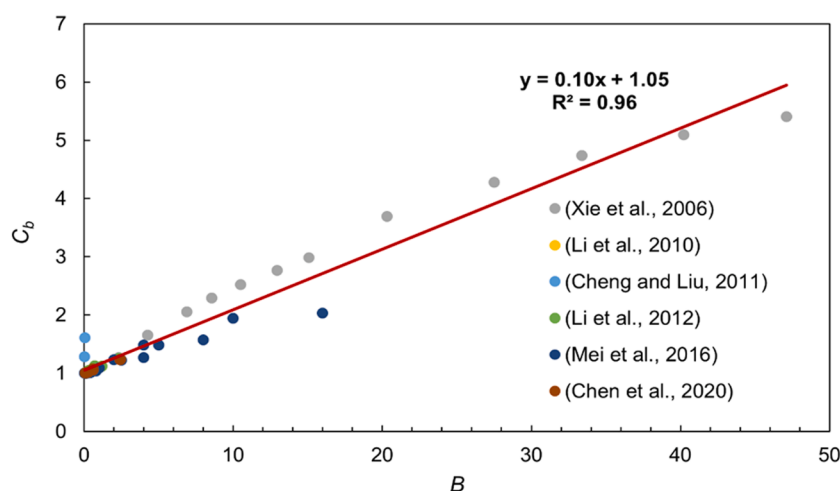


Fig. 4. Correlations between the buoyancy parameter B and the buoyancy coefficient C_b inside a street canyon with heated bottom surfaces.

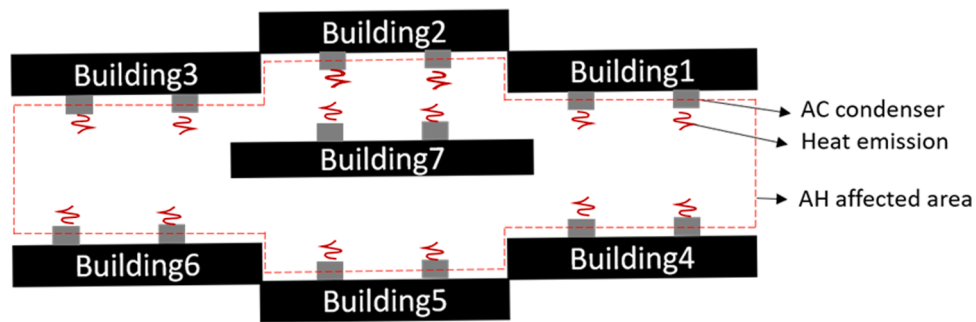


Fig. 5. Schematic of AH emission from seven buildings in the study area.

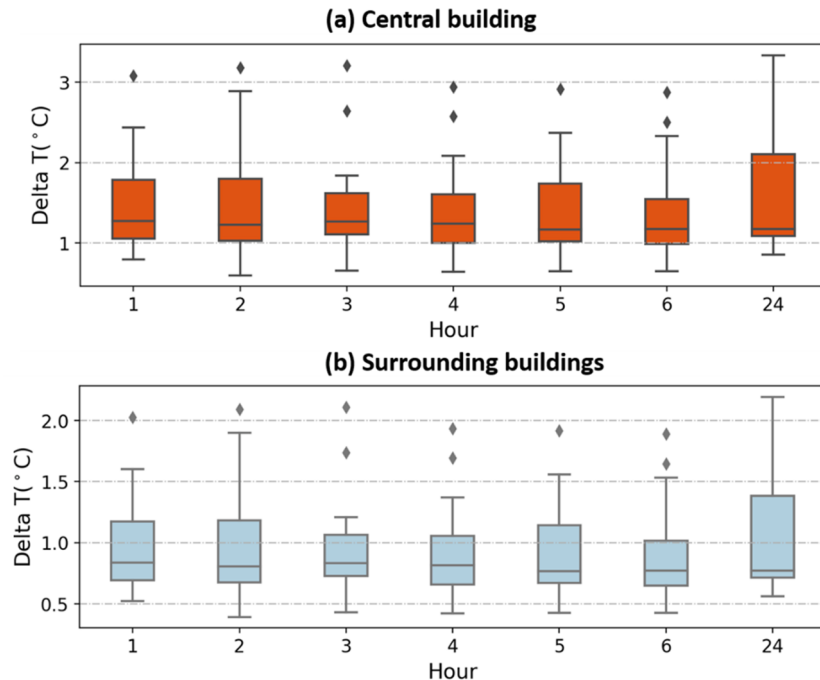


Fig. 6. Distributions of modelled hourly temperature increments around the (a) central building and (b) surrounding buildings.

While the air temperature from the developed microclimate data (Dataset III) was spatially averaged rather than single-point measurement. Besides, the impact of wind speed on energy consumption was insignificant, compared with that of air temperature.

Furthermore, the daily mean dry-bulb temperatures from five weather datasets were compared, as shown in Fig. 8. The daily mean temperatures in TMY data were lower than those in other datasets, especially in the latter half month of June 2015, indicating a warming trend in the past two decades. The daily mean temperatures in the developed microclimate data were the highest among the latter four datasets (Datasets B, I-III), followed by those measured at the urban ground, suburban ground, and urban rooftop.

5. Results and discussion

To validate the energy simulation models, both monthly and hourly energy consumptions in the target buildings in June 2015 were analyzed, by comparing the simulated results with the actual energy consumption data. The actual monthly energy consumption of each target building was obtained by multiplying the monthly energy consumption per household (Energy Market Authority, 2015) with the number of flats in each building (Government of Singapore, 2019). The monthly data was further downscaled to generate the hourly energy

consumption profile, based on the typical weekly and daily electricity load profiles presented in a previous study in Singapore (Quah & Roth, 2012). It is worth noting that the analysis in this study is restricted to weekdays, due to the lack of reliable data on residents' occupancy level and behavior on weekends.

5.1. Monthly energy prediction

Fig. 9(a) shows the actual total monthly energy consumption (Baseline) of seven buildings and modelling results (Cases I-V) using the above mentioned five weather datasets. All the energy consumption sources, e.g., AC systems and household appliances, were included at this analysis. First, it is observed that the prediction error (i.e., relative error) of the total monthly energy consumption decreased from 12% to 6% when the adopted weather data shifted from Dataset A (TMY data) to Dataset III (the developed microclimate data). The implementation of Dataset III contributed to the lowest prediction error at BEM. Secondly, the total monthly energy prediction using the Dataset I (measured at the urban rooftop) was less accurate than the one using Dataset B (measured at the suburban ground). This suggests that the microclimate data measured at high urban rooftops might not be suitable for BEM, as they are not representative for weather conditions in the deep urban canyon. Lastly, the total monthly energy consumption simulated using Dataset III

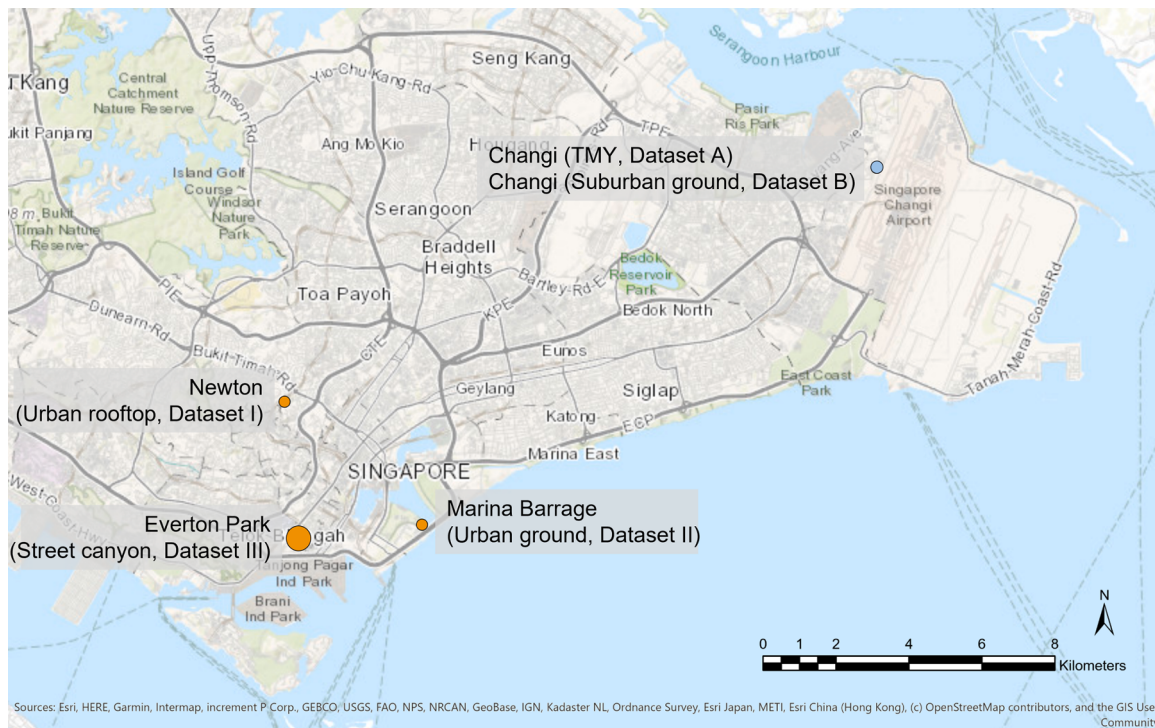


Fig. 7. Locations of the weather datasets used. Five weather datasets are included, the historical TMY (Dataset A), measured data from an airport meteorological station (Dataset B), and three microclimate datasets, i.e., measured microclimate data (Datasets I and II), and developed microclimate data (Dataset III).

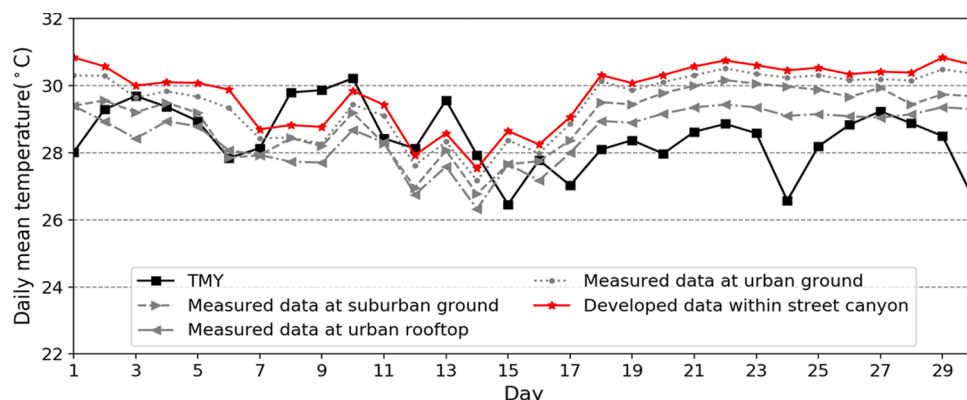


Fig. 8. Daily mean ambient temperatures from five weather datasets, including the TMY (Dataset A), measured data from an airport meteorological station (Dataset B, at the suburban ground), and three microclimate datasets, i.e., measured data at a meteorological station (Dataset I, at the urban rooftop), measured data at a meteorological station (Dataset II, at the urban ground), and developed microclimate data (Dataset III, within the street canyon).

were more accurate than the one using Dataset II, since the impact of anthropogenic heat on air temperature is included in Dataset III. Fig. 9 (b) shows the cross-comparison results during AC operation hours (23:00–6:00). Similar to the trends observed in Fig. 9(a), the predictions using Dataset A underestimated the total energy consumption 18% during AC operation hours on weekdays, and the prediction error using Dataset III is the smallest, only 2%.

Fig. 10 shows the simulated monthly cooling loads of seven buildings using five weather datasets on the weekdays of June 2015. Among five cases, the predicted cooling load using Dataset A (TMY data) at Case I was the lowest, with the differences of 8%, 3%, 18%, and 25% respectively, when compared to the predictions in Cases II–V. This further proves that the simulated cooling loads of urban high-density residential buildings using the TMY data would be lower than those using the measured or developed weather dataset. In other words, urban weather data, especially the representative weather data (i.e., developed

microclimate data), has a significant impact on the cooling demands of residential buildings in high-density urban areas.

In summary, BEM performance for residential buildings in urban dense areas is sensitive to the input weather data. The TMY data tends to underestimate the ambient air temperatures within the street canyon and thus underestimate the indoor cooling demand. Compared with the measured microclimate data at the urban ground, the usage of weather data measured at an urban high-rise rooftop or less densely built areas (e.g., suburban ground) tends to underestimate the cooling demand of residential buildings in high-density urban areas as well. The best weather data for BEM is found to be the developed microclimate data (Dataset III), which is integrated by measured microclimate data at urban ground (Dataset II) and the modelled air temperature increments due to AH emission from AC systems.

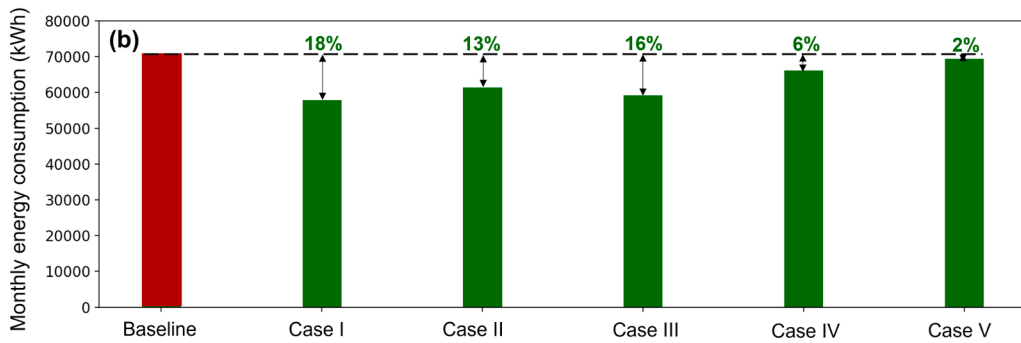
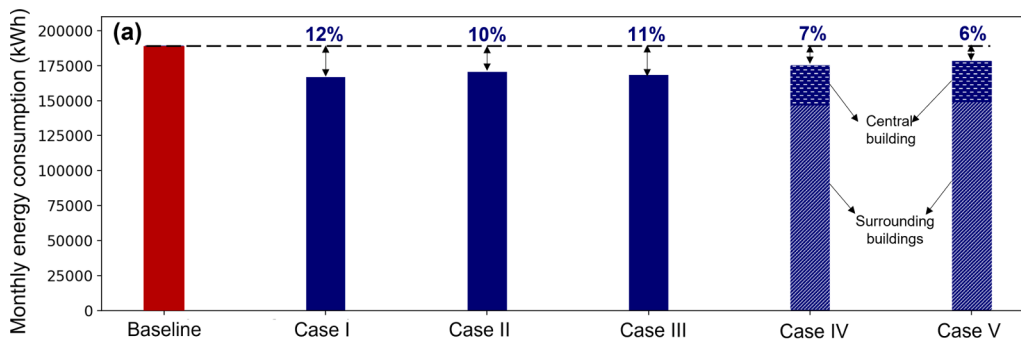


Fig. 9. (a). Comparisons between the actual total monthly energy consumption (Baseline) and modelling results (Cases I-V) using five different input weather datasets. Baseline represents the actual total monthly energy consumption (Source: Energy Market Authority (EMA), 2015). Cases I-V represent the simulated total monthly energy consumptions using Dataset A (TMY data), Dataset B (measured weather data at the suburban ground), and microclimate data, i.e., Dataset I (measured at the urban rooftop), Dataset II (measured at the urban ground), and Dataset III (developed microclimate data), respectively. (b). Comparisons between the actual total monthly energy consumption (Baseline) and modelling results (Cases I-V) during AC operation hours (23:30–6:00).

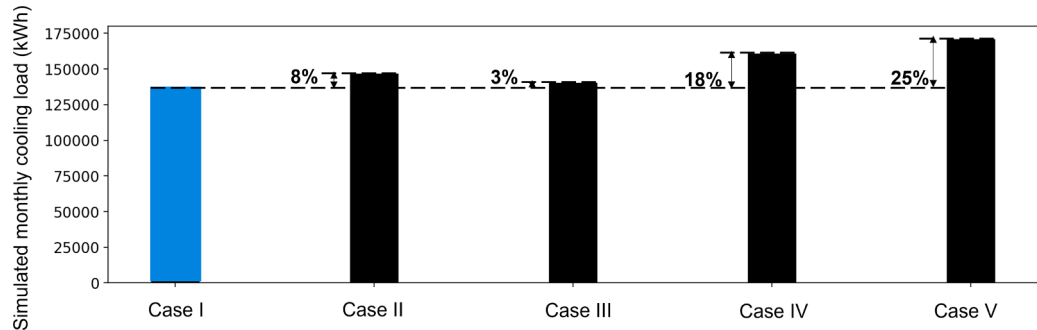


Fig. 10. Simulated monthly cooling loads of seven buildings using five different weather datasets on the weekdays of June 2015. Cases I-V represent the simulated monthly cooling loads using Dataset A (TMY data), Dataset B (measured weather data at the suburban ground), and microclimate data, i.e., Dataset I (measured at the urban rooftop), Dataset II (measured at the urban ground), and Dataset III (developed microclimate data), respectively.

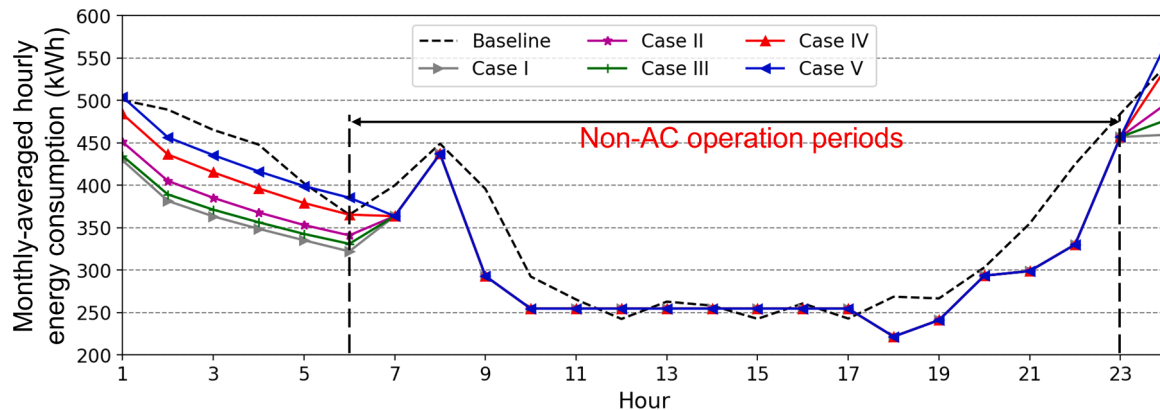


Fig. 11. Comparisons between the actual energy consumption (Baseline) and simulated monthly-averaged hourly energy consumptions (Cases I-V) using five different weather datasets during 24 hours of the weekdays of June 2015. The baseline represents the MAHE consumption (Source: EMA, 2015). Cases I-V represent the simulated MAHE consumptions using Dataset A (TMY data), Dataset B (measured weather data at the suburban ground), and microclimate data, i.e., Dataset I (measured at the urban rooftop), Dataset II (measured at the urban ground), and Dataset III (developed microclimate data), respectively.

5.2. Hourly energy prediction

Fig. 11 shows the actual and simulated monthly-averaged hourly energy (MAHE) consumptions for seven buildings on the weekdays of June 2015. The MAHE consumption is defined as the mean value of the energy consumptions at a particular hour of a certain month. During the AC operation hours, the simulated MAHE consumptions using the developed microclimate data at Case V best matched the actual profile (i.e., Baseline), with an averaged difference of 7 kWh. In contrast, the simulated MAHE consumptions using TMY data at Case I showed the largest deviation from Baseline, with an averaged difference of 81 kWh. During non-AC operation hours, all the simulated MAHE consumptions well agreed with the actual profile. It indicates that the difference among Cases I-V is only caused by the impact of air temperature on cooling load, but not other household appliances.

Furthermore, two performance indexes were adopted to evaluate the impacts of five different weather datasets on BEM and validate the developed energy models. The two indexes, i.e., mean bias error (MBE) and coefficient of variation of root mean square error (CVRMSE), are calculated by Eq. (8) and Eq. (9) respectively.

$$MBE = \frac{\sum_{i=1}^N (E_i^{act} - E_i^{pre})}{\sum_{i=1}^N E_i^{act}} \times 100\% \quad (8)$$

$$CVRMSE = \frac{\sqrt{\sum_{i=1}^N (E_i^{act} - E_i^{pre})^2 / N}}{\sum_{i=1}^N E_i^{act} / N} \times 100\% \quad (9)$$

where E_i^{act} is the actual hourly building energy consumption, in kWh; E_i^{pre} is the predicted hourly building energy consumption, in kWh; i is a certain hour; and N is the number of hours in a certain period (e.g., a month or a day). Building energy models are generally considered well-validated if the MBE is less than 10% and CVRMSE is less than 30% (ASHRAE, 2002).

The MBE and CVRMSE in the hourly energy consumption predictions of seven buildings using five different weather datasets at Cases I-V are listed in **Table 6**. All the CVRMSEs at 5 Cases were less than 30%. However, only the MBEs at Cases IV and V were less than 10%. It indicates that the measured microclimate data at the urban ground and the developed microclimate data are acceptable for BEM. This analysis result is consistent with the aforementioned analysis of monthly energy predictions.

6. Implementations for climate resilience

Based on the above results and discussion, the most representative weather data for BEM is the developed microclimate data (Dataset III), which is developed by the new framework in this study. In this section, the developed framework was applied to estimate and anticipate the residential energy consumptions under the short-term COVID pandemic and long-term climate change scenarios. This implementation study is to support decision-making in the future urban energy planning for urban climate resilience.

6.1. Short-term scenario: COVID pandemic

The COVID-19 pandemic has significantly changed urban residents' lifestyles. In March 2020, the Singapore government issued a 'circuit

Table 6
BEM performances using different weather datasets.

	Case I	Case II	Case III	Case IV	Case V
MBE	12%	10%	11%	7%	6%
CVRMSE	19%	17%	18%	15%	15%

Note: Cases I-V represent the simulated hourly energy consumptions.

breaker' lockdown policy to curb the spread of coronavirus disease. From April to June 2020, all the residents were required to work from home to avoid gathering at workplaces. The daily residential energy consumption profiles thus changed significantly. In this section, we estimated the impact of COVID pandemic on the energy consumption at residential buildings using the new weather data development framework. The energy consumption modelling under two scenarios (i.e., COVID pandemic scenario and normal scenario) was conducted for the cross-comparison. The microclimate data under the normal scenario were from Case V in Section 5. Under the COVID pandemic scenario, AC operation hours on the weekdays were assumed to be prolonged during the daytime. Specifically, AC systems were turned on during 9:00–12:00 and 13:00–17:00 to provide a productive working environment. In addition, AC systems were still turned on during 23:30–6:00 to provide a comfortable sleeping environment. Accordingly, the microclimate data under the COVID pandemic scenario was developed by integrating the measured weather data at the urban ground (at Marina Barrage) and updated modelled air temperature increments due to prolonged AC operation hours.

Fig. 12(a) and (b) show the distributions of modelled air temperature increments under the COVID pandemic scenario for the central building and surrounding buildings, respectively. It is observed that the medians of the hourly air temperature increments ranged from 0.73°C to 1.42°C around the central building and from 0.47°C to 0.93°C around the surrounding buildings. The maximum temperature increment occurred at 10:00, with the maximum values of about 3.0°C for the central building and 2.0°C for the surrounding buildings.

Fig. 13(a) and (b) show the estimated total monthly energy consumptions of the central building and surrounding buildings respectively under the COVID pandemic scenario and the normal scenario. Estimated total monthly energy consumptions of the central building (35,530 kWh) and surrounding buildings (186,469 kWh) under the COVID pandemic scenario increased 20% and 25% respectively, compared with the normal scenario.

Fig. 13(c) shows the estimated total monthly energy consumption (222,000 kWh) of all the buildings under the COVID pandemic scenario increased 24%, compared with the one (179,050 kWh) under the normal scenario. The estimated increase (24%) of energy consumption is comparable to the actual value 22% (Energy Market Authority, 2021).

Fig. 13(d) shows the estimated total monthly energy consumptions of all the buildings during the AC operation hours under the COVID pandemic and normal scenarios. An increase of 118% (i.e., from the normal situation of 69,612 kWh to the COVID situation of 151,785 kWh) was observed, due to prolonged AC operation hours during the daytime. It indicates that the work-from-home mode would pose a potential risk to residential power suppliers and even endanger the grid safety due to doubled cooling energy demands.

To further investigate the peak demands, the estimated monthly-averaged hourly energy (MAHE) consumptions under the COVID pandemic and normal scenarios were compared, as shown in **Fig. 14(a)**. It was observed that the peak hour, 10:00, under the COVID pandemic scenario was different from the one, 24:00, under the normal scenario. **Fig. 14(b)** shows the monthly variations of the estimated energy consumption at the peak hour (10:00 under the COVID pandemic scenario and 24:00 under the normal scenario). The maximum peak hour energy consumption (16th Workday, 817 kWh) under the COVID pandemic scenario was 21% larger than the one (16th Workday, 676 kWh) under the normal scenario. This large increase might pose potential risks for power grid operations during the new peak hours when the work-from-home becomes the new normal in the post-pandemic period.

6.2. Long-term scenario: Climate change

In this section, we anticipated the impact of climate change on the energy consumption at residential buildings using the new weather data development framework. The energy consumption modelling under two

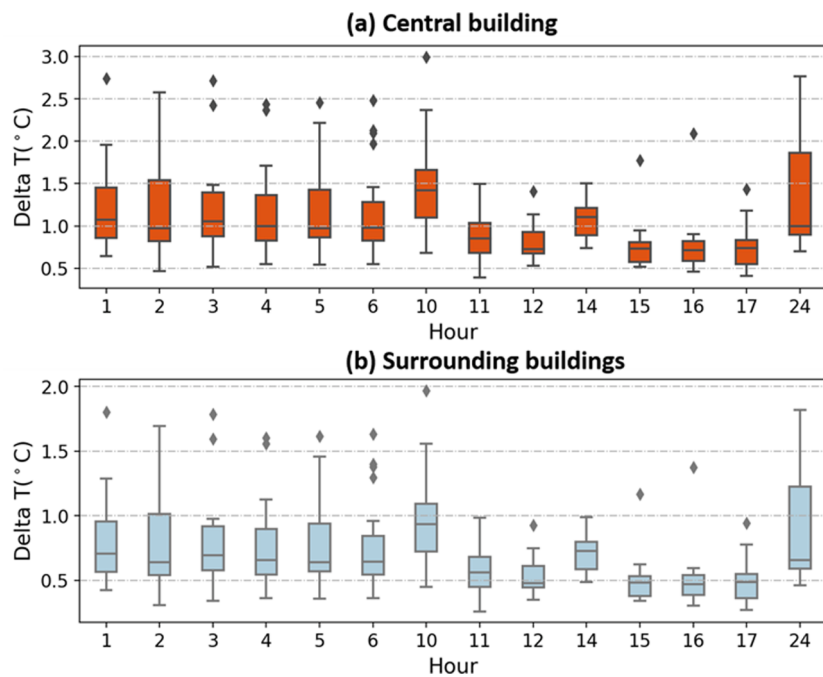


Fig. 12. Distributions of modelled hourly air temperature increments around the (a) central building and (b) surrounding buildings under the COVID pandemic scenario.

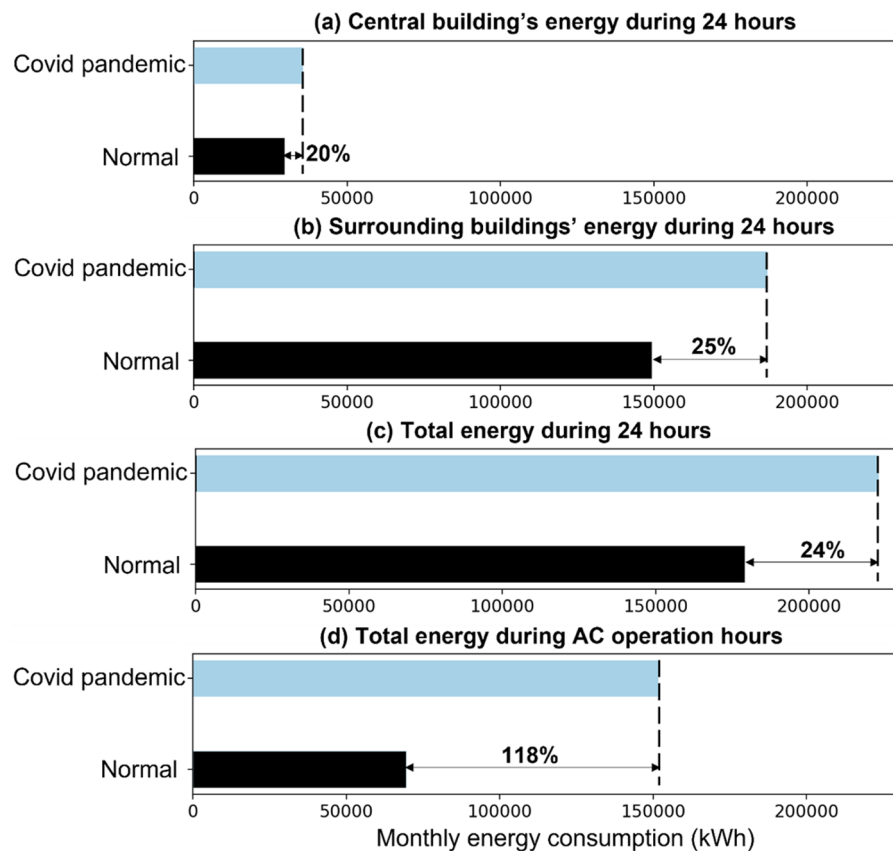


Fig. 13. Estimated total monthly energy consumptions under the COVID pandemic and normal scenarios of the (a) central building, (b) surrounding buildings, (c) all the buildings, and (d) all the buildings during AC operation hours on the weekdays of June.

scenarios (i.e., climate change scenario in 2030s and normal scenario in 2015) was conducted for the cross-comparison. The microclimate data under the normal scenario were from Case V in Section 5. The

microclimate data under the climate change scenario were developed at two steps: Step 1, we included the impact of climate change on air temperature and chose an extreme climate scenario (RCP 8.5), under

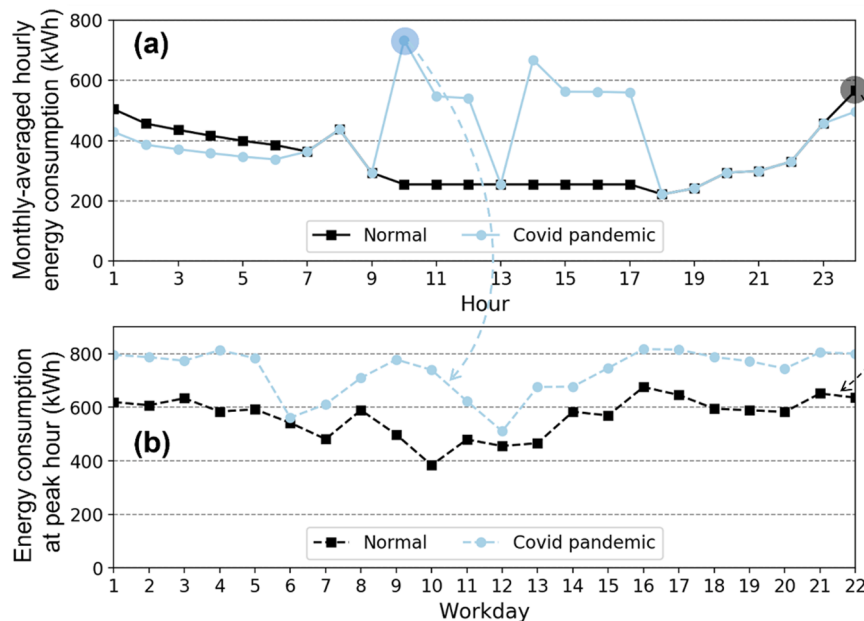


Fig. 14. Estimated hourly energy consumptions under the COVID pandemic and normal scenarios: (a) monthly-averaged hourly energy consumptions and (b) monthly variations of energy consumptions at the peak hour (10:00 under the COVID scenario and 24:00 under the normal scenario).

which the ambient air temperature was predicted to increase 1°C in the 2030s (Marzin et al., 2015); Step 2, we added up another air temperature increments caused by anthropogenic heat. It should be noted that energy consumption modelling under the two scenarios only differs in the weather data. The operation schedules of all the electric equipment (including AC systems) were kept the same.

Fig. 15(a) and (b) show the distributions of modelled air temperature increments under the climate change scenario for the central building and surrounding buildings, respectively. It is observed that the medians of the hourly air temperature increments ranged from 2.53°C to 2.71°C around the central building and from 2.04°C to 2.16°C around

surrounding buildings. The largest air temperature increment occurred at 24:00, with the maximum values of 5.0°C for the central building and 3.7°C for surrounding buildings.

Fig. 16(a) and (b) show the anticipated total monthly energy consumptions of the central building and surrounding buildings respectively in 2015 (normal scenario) and 2030s (climate change scenario). The developed microclimate data were applied in this analysis. Anticipated total monthly energy consumptions of the central building (31,015 kWh) and surrounding buildings (29,628 kWh) under the climate change scenario increased 4.6 % and 6.2% respectively, compared with the normal scenario in 2015.

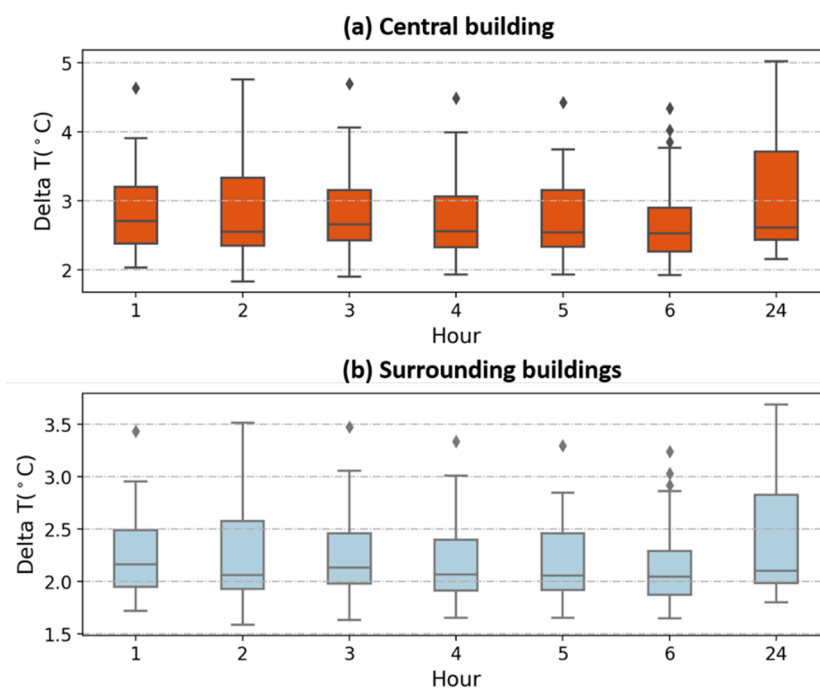


Fig. 15. Distributions of modelled hourly air temperature increments around the (a) central building and (b) surrounding buildings under the climate change scenario.

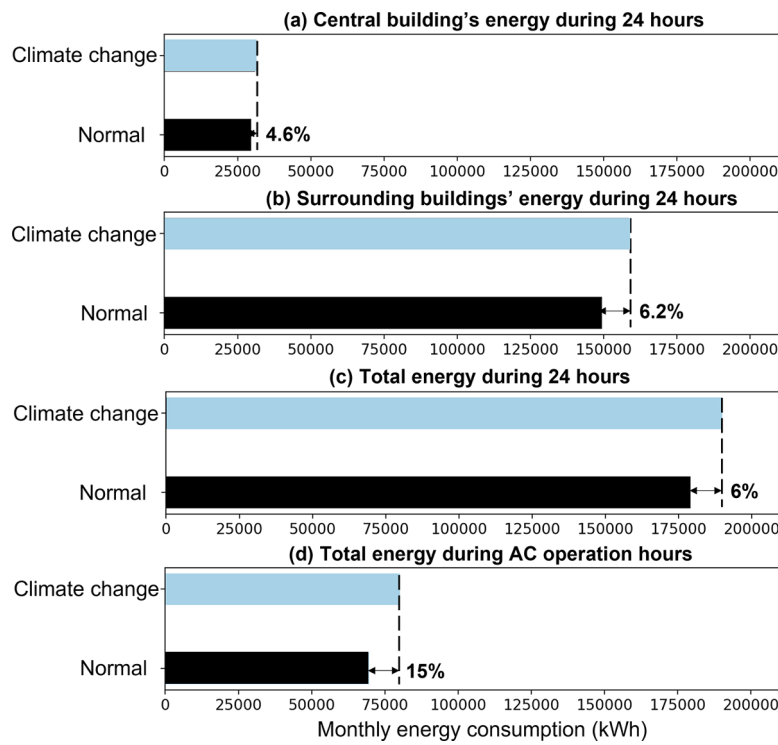


Fig. 16. Anticipated total monthly energy consumptions under the climate change and normal scenarios of the (a) central building, (b) surrounding buildings (c) all the buildings, and (d) all the buildings during AC operation hours on the weekdays of June.

Fig. 16(c) shows that the anticipated total monthly total energy consumption (189,695 kWh) of all the buildings under the climate change scenario increased 6%, compared with the one (179,050 kWh) under the normal scenario.

Fig. 16(d) shows the anticipated total monthly energy consumption of all the buildings during AC operation hours under the climate change and normal scenarios. An increase of 15% (i.e., from the normal situation of 69,612 kWh to the climate change situation of 80,257 kWh) was

observed. It indicates that climate change might increase the burden on residential electricity suppliers in the future.

To further investigate the peak demands, the anticipated monthly-averaged hourly energy (MAHE) consumptions under climate change and normal scenarios were compared, as shown in Fig. 17(a). It was observed that the peak hour, 24:00, was the same under both climate change and normal scenarios. This is mainly due to the same AC operation schedule. Fig. 17(b) shows the monthly variations of the

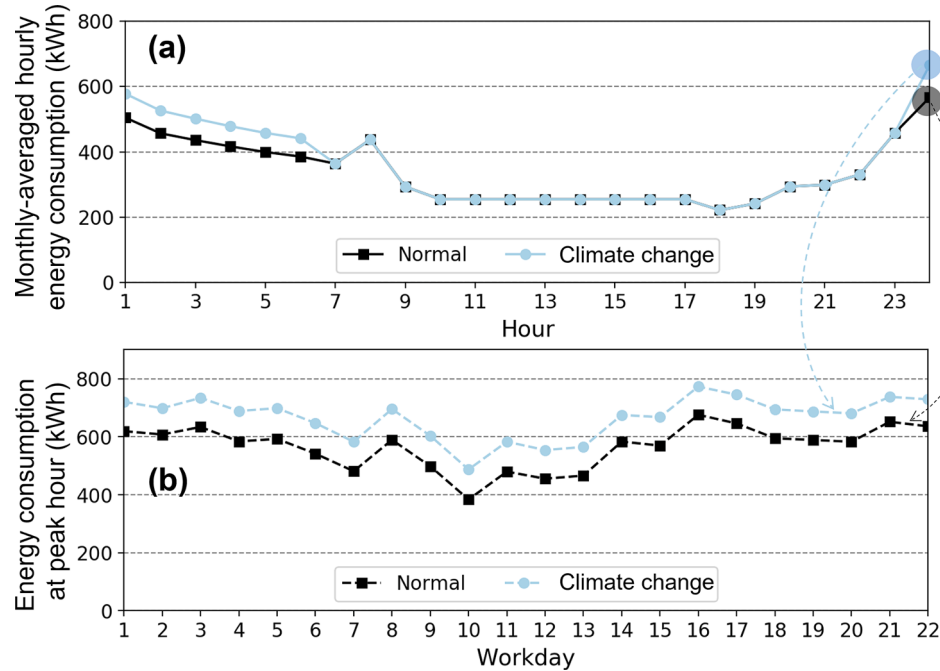


Fig. 17. Anticipated hourly energy consumptions under the climate change and normal scenarios: (a) monthly-averaged hourly energy consumptions and (b) monthly variations of energy consumptions at the peak hour, 24:00.

anticipated energy consumption at the peak hour. The maximum peak hour energy consumption (16th Workday, 773 kWh) under the climate change scenario was 14% larger than the one (16th Workday, 676 kWh) under the normal scenario. This significant increase might be risky for the power grid safety in the 2030s and needs to be addressed during urban resilience planning.

7. Conclusions and future study

This study investigates the impacts of input weather data on building energy modelling (BEM) performance for high-density residential buildings in the tropical climate. The studied weather datasets include TMY data, data measured near the airport (suburban ground), and three microclimate datasets i.e., i) data measured at a high-rise rooftop near the site, ii) data measured at the near-ground open space close to the site, and iii) developed microclimate data within the urban canopy layer at the site. A cross-comparison study is conducted using real energy consumption data, and the analysis results indicate that the developed microclimate data are the best for BEM in high-density urban areas. Using the new framework to develop input weather data, we estimate and anticipate residential energy consumptions under two scenarios, i.e., i) short-term COVID pandemic scenario and ii) long-term climate change scenario. The following conclusions are drawn from this study:

- New microclimate data are developed by integrating the measured near-ground weather data and microclimate modelling results by a practical GIS tool.
- BEM performance is sensitive to the input weather data. Among the five weather datasets, the developed microclimate data performs the best at BEM, decreasingly followed by the measured microclimate data at the urban ground (Dataset II), measured weather data at the suburban ground (Dataset B), measured microclimate data at the urban rooftop (Dataset I), and TMY data (Dataset A).
- Quantitative evaluation of BEM performance is conducted at various time scales. The prediction error of the total monthly energy consumption decreases from 12% to 6% when the adopted weather dataset shifts from TMY data to developed microclimate data. The prediction error of the hourly energy consumption is very small, 6% (MBE) and 15% (CVRMSE), using the developed microclimate data.
- Cross-comparison of BEM performances using three measured weather datasets (i.e., Dataset B measured at the suburban ground, Dataset I measured at the urban rooftop, and Dataset II measured at the urban ground) is conducted. The results on BEM performances indicate that Dataset II is more representative to the reality and better than Datasets I and B.
- Under the short-term COVID pandemic scenario, the estimated total monthly energy consumption increases 24% compared with the one under the normal scenario, and it increases 118% when only the AC operation hours are considered. Besides, the maximum peak hour energy consumption under the COVID pandemic scenario increases 21% compared with the one under the normal scenario. Moreover, the occurrence of the peak energy consumption shifts from nighttime under the normal scenario to daytime under the COVID scenario. Such changes and energy usage increases would pose potential risks to the grid safety during the post-pandemic period if the work-from-home became the new normal.
- Under the long-term climate change scenario, the anticipated total monthly energy consumption increases 6% compared with the one under the normal scenario, and it increases 15% when only the AC operation hours are considered. Moreover, the maximum peak hour energy consumption under the climate change scenario increases 14% compared with the one under the normal scenario. This long-term increase in residential energy usage needs to be addressed during urban resilience planning.

There are several limitations in this study, and we will address them

in the future. Firstly, we will investigate the model sensitivity to building parameters, such as coefficient of performance (COP) and air change per hour (ACH), to further improve the performance of BEM. Secondly, we used the real monthly energy consumption data for model validation and will use the real hourly energy consumption data to improve the model validation when such data become available. Thirdly, the new microclimate data development framework was applied at BEM for residential buildings located in high-density urban areas. In the future, residential buildings located in medium- and low-density urban areas will be also studied to evaluate various sensitivity of BEM performance on weather data. Fourthly, a simplified and identical AC operation schedule was assumed for all the households in the COVID pandemic analysis. This can be improved by adopting a realistic AC operation profile in the future based on survey data during the COVID period. Last but not least, the other climate change scenarios (e.g., RCP 2.6, RCP 4.5, and RCP 6) could be considered to provide more comprehensive information with higher confidence to improve urban climate resilience.

Declaration of Competing Interest

The authors declare that they have no known competing financial interests or personal relationships that could have appeared to influence the work reported in this paper.

Acknowledgements

This research project is financially supported by Singapore National Research Foundation, Singapore ETH centre, Future Resilience System II grant (Grant no. R-295-000-176-592), and Singapore Ministry of Education, NUS Presidential Young Professorship (Grant no. R-295-000-172-133). The authors would also like to thank the Energy Market Authority (EMA), National Environment Agency (NEA), and Housing & Development Board (HDB) for providing access to the actual energy consumption data, measured weather data, and floor plans of studied buildings respectively.

References

- Abergel, T., Delmastro, C., & Kevin, L. (2020). *Buildings—The COVID-19 crisis and clean energy progress*. Paris, France: International Energy Agency.
- Ascione, F., Bianco, N., Iovane, T., Mastellone, M., & Mauro, G. M. (2020). Is it fundamental to model the inter-building effect for reliable building energy simulations? Interaction with shading systems. *Building and Environment*, 183, Article 107161.
- ASHRAE. (2002). *Guideline 14-2002: Measurement of energy and demand savings*. Atlanta: ASHRAE.
- Auffhammer, M., Baylis, P., & Hausman, C. H. (2017). Climate change is projected to have severe impacts on the frequency and intensity of peak electricity demand across the United States. *Proceedings of the National Academy of Sciences*, 114(8), 1886–1891.
- Balasco, P., Bonte, L., Frigati, L., Humbert, P., Martin, A., & Sizarine, V. (2010). Practical guide for clinicians, nurse, laboratory technicians and medical auxiliaries. *Medecins sans frontieres*. Belgium: UK WHO.
- Bianchi, C., & Smith, A. D. (2019). Localized Actual Meteorological Year File Creator (LAF): A tool for using locally observed weather data in building energy simulations. *SoftwareX*, 10, Article 100299.
- Bouyer, J., Inard, C., & Musy, M. (2011). Microclimatic coupling as a solution to improve building energy simulation in an urban context. *Energy and Buildings*, 43, 1549–1559.
- Brueisauer, M., Meggers, F., Saber, E., Li, C., & Leibundgut, H. (2014). Stuck in a stack—Temperature measurements of the microclimate around split type condensing units in a high rise building in Singapore. *Energy and Buildings*, 71, 28–37.
- Bueno, B., Norford, L., Hidalgo, J., & Pigeon, G. (2013). The urban weather generator. *Journal of Building Performance Simulation*, 6(4), 269–281.
- Building and Construction Authority. (2001). *Code on Envelope Thermal Performance for Buildings*.
- Building and Construction Authority. (2016). *GM RB 2016: Green Mark for Residential Buildings*.
- Catalina, T., Virgone, J., & Blanco, E. (2008). Development and validation of regression models to predict monthly heating demand for residential buildings. *Energy and Buildings*, 40(10), 1825–1832.
- Chan, A. (2011). Developing a modified typical meteorological year weather file for Hong Kong taking into account the urban heat island effect. *Building and Environment*, 46(12), 2434–2441.

- Chen, G., Rong, L., & Zhang, G. (2020). Comparison of urban airflow between solar-induced thermal wall and uniform wall temperature boundary conditions by coupling CitySim and CFD. *Building and Environment*, 172, Article 106732.
- Cheng, W. C., Liu, C. H., & Leung, D. Y. C. (2009). On the comparison of the ventilation performance of street canyons of different aspect ratios and Richardson number. *Building Simulation*, 2(1), 53–61.
- Chua, K., & Chou, S. (2010). Energy performance of residential buildings in Singapore. *Energy*, 35(2), 667–678.
- Ciancio, V., Falasca, S., Golasi, I., Curci, G., Coppi, M., & Salata, F. (2018). Influence of input climatic data on simulations of annual energy needs of a building: EnergyPlus and WRF modeling for a case study in Rome (Italy). *Energies*, 11(10), 2835.
- Congedo, P. M., Baglivo, C., Seyhan, A. K., & Marchetti, R. (2021). Worldwide dynamic predictive analysis of building performance under long-term climate change conditions. *Journal of Building Engineering*, 42, Article 103057.
- Crawley, D. B., Lawrie, L. K., Winkelmann, F. C., Buhl, W. F., Huang, Y. J., Pedersen, C. O., ... & Glazer, J. (2001). EnergyPlus: creating a new-generation building energy simulation program. *Energy and Buildings*, 33(4), 319–331.
- Dong, B., Cao, C., & Lee, S. E. (2005). Applying support vector machines to predict building energy consumption in tropical region. *Energy and Buildings*, 37(5), 545–553.
- Duarte, C., Raftery, P., & Schiavon, S. (2018). Development of whole-building energy models for detailed energy insights of a large office building with green certification rating in singapore. *Energy Technology*, 6(1), 84–93.
- Energy Market Authority. (2015a). *Singapore energy statistics 2015*. https://www.ema.gov.sg/cmsmedia/Publications_and_Statistics/Publications/SES2015_Final_website_2mb.pdf.
- Energy Market Authority. (2015b). *Average monthly household electricity consumption by postal code (public housing) & dwelling type in 2015*. https://www.ema.gov.sg/statistics.aspx?Sta_id=20150617kEhn53Jk6sDQ.
- Energy Market Authority. (2021). *Electricity demand (Circuit Breaker)*. <https://www.ema.gov.sg/electricity-demand-circuit-breaker.aspx>.
- Farrow, H. (2020). *Commercial down v residential up: COVID-19's electricity impact*.
- Founda, D., & Santamouris, M. (2017). Synergies between urban heat island and heat waves in Athens (Greece), during an extremely hot summer (2012). *Scientific Reports*, 7(1), 1–11.
- Fumo, N., Mago, P., & Luck, R. (2010). Methodology to estimate building energy consumption using EnergyPlus Benchmark Models. *Energy and Buildings*, 42(12), 2331–2337.
- Gobakis, K., & Kolokotsa, D. (2017). Coupling building energy simulation software with microclimatic simulation for the evaluation of the impact of urban outdoor conditions on the energy consumption and indoor environmental quality. *Energy and Buildings*, 157, 101–115.
- Government of Singapore. (2019). *HDB property information*. <https://storage.data.gov.sg/hdb-property-information/resources/hdb-property-information-2019-07-05T01-29-20Z.csv>.
- Hong, T., Chen, Y., Luo, X., Luo, N., & Lee, S. H. (2020). Ten questions on urban building energy modeling. *Building and Environment*, 168, Article 106508.
- Housing & Development Board. (2021). *Residential floor plan*. <https://services2.hdb.gov.sg/webapp/BC31ISOP2/BC31SMMain>.
- Ignatiou, M., Wong, N. H., & Jusuf, S. K. (2016). The significance of using local predicted temperature for cooling load simulation in the tropics. *Energy and Buildings*, 118, 57–69.
- International Energy Agency. (2020). *Tracking buildings 2020*. Retrieved from <https://www.iea.org/reports/tracking-buildings-2020>.
- International Energy Agency. (2021). *Global energy review 2021*. Retrieved from <https://iea.blob.core.windows.net/assets/d0031107-401d-4a2f-a48b-9eed19457335/GlobalEnergyReview2021.pdf>.
- Jabareen, Y. (2013). Planning the resilient city: Concepts and strategies for coping with climate change and environmental risk. *Cities*, 31, 220–229.
- Jamei, E., Ossen, D., Seyedmahmoudian, M., Sandanayake, M., Stojcevski, A., & Horan, B. (2020). Urban design parameters for heat mitigation in tropics. *Renewable and Sustainable Energy Reviews*, 134, Article 110362.
- Jiang, P., Van Fan, Y., & Klemeš, J. J. (2021). Impacts of COVID-19 on energy demand and consumption: Challenges, lessons and emerging opportunities. *Applied Energy*, 285, Article 116441.
- Jusuf, S. K., & Wong, N. H. (2009). Development of empirical models for an estate level air temperature prediction in Singapore. In *Proceedings of the second international conference on countermeasures to urban heat islands*.
- Kohler, M., Blond, N., & Clappier, A. (2016). A city scale degree-day method to assess building space heating energy demands in Strasbourg Eurometropolis (France). *Applied Energy*, 184, 40–54.
- Kolokotroni, M., & Giridharan, R. (2008). Urban heat island intensity in London: An investigation of the impact of physical characteristics on changes in outdoor air temperature during summer. *Solar Energy*, 82(11), 986–998.
- Kolokotroni, M., Ren, X., Davies, M., & Mavrogiani, A. (2012). London's urban heat island: Impact on current and future energy consumption in office buildings. *Energy and Buildings*, 47, 302–311.
- Li, W., Zhou, Y., Cetin, K., Eom, J., Wang, Y., Chen, G., & Zhang, X. (2017). Modeling urban building energy use: A review of modeling approaches and procedures. *Energy*, 141, 2445–2457.
- Li, X. X., Britter, R. E., Norford, L. K., Koh, T. Y., & Entekhabi, D. (2012). Flow and pollutant transport in urban street canyons of different aspect ratios with ground heating: Large-eddy simulation. *Boundary-Layer Meteorology*, 142(2), 289–304.
- Li, X., Zhou, Y., Yu, S., Jia, G., Li, H., & Li, W. (2019a). Urban heat island impacts on building energy consumption: A review of approaches and findings. *Energy*, 174, 407–419.
- Li, X. X., Britter, R. E., Koh, T. Y., Norford, L. K., Liu, C. H., Entekhabi, D., & Leung, D. Y. (2010). Large-eddy simulation of flow and pollutant transport in urban street canyons with ground heating. *Boundary-Layer Meteorology*, 137(2), 187–204.
- Li, Z., Quan, S. J., & Yang, P. P.-J. (2016). Energy performance simulation for planning a low carbon neighborhood urban district: A case study in the city of Macau. *Habitat International*, 53, 206–214.
- Liu, Y., Stouffs, R., Tablada, A., Wong, N. H., & Zhang, J. (2017). Comparing micro-scale weather data to building energy consumption in Singapore. *Energy and Buildings*, 152, 776–791.
- Luo, X., Oyedele, L. O., Ajayi, A. O., Monyei, C. G., Akinade, O. O., & Akanbi, L. A. (2019). Development of an IoT-based big data platform for day-ahead prediction of building heating and cooling demands. *Advanced Engineering Informatics*, 41, Article 100926.
- Madlener, R., & Sunak, Y. (2011). Impacts of urbanization on urban structures and energy demand: What can we learn for urban energy planning and urbanization management? *Sustainable Cities and Society*, 1(1), 45–53.
- Martin, M., Wong, N. H., Hii, D. J. C., & Ignatiou, M. (2017). Comparison between simplified and detailed EnergyPlus models coupled with an urban canopy model. *Energy and Buildings*, 157, 116–125.
- Marzin, C., Rahmat, R., Bernie, D., Bricheno, L., Buonomo, E., Calvert, D., et al. (2015). *Singapore's second national climate change study—Phase 1*. E. Met Office, UK, Centre for Climate Research Singapore, S., National Oceanography Centre, L., UK, CSIRO, A. & Newcastle University, N., UK (ed).
- Mei, S. J., Liu, C. W., Liu, D., Zhao, F. Y., Wang, H. Q., & Li, X. H. (2016). Fluid mechanical dispersion of airborne pollutants inside urban street canyons subjecting to multi-component ventilation and unstable thermal stratifications. *Science of The Total Environment*, 565, 1102–1115.
- Mei, S. J., & Yuan, C. (2021). Analytical and numerical study on transient urban street air warming induced by anthropogenic heat emission. *Energy and Buildings*, 231, Article 110613.
- Miller, C., Thomas, D., & Kämpf, J. (2018). & Schlüter A. Urban and building multiscale co-simulation: Case study implementations on two university campuses. *Journal of Building Performance Simulation*, 11(3), 309–321.
- Mirzaei, P. A. (2015). Recent challenges in modeling of urban heat island. *Sustainable Cities and Society*, 19, 200–206.
- Mo, H., Sun, H., Liu, J., & Wei, S. (2019). Developing window behavior models for residential buildings using XGBoost algorithm. *Energy and Buildings*, 205, Article 109564.
- Mocanu, E., Nguyen, P. H., Gibescu, M., & Kling, W. L. (2016). Deep learning for estimating building energy consumption. *Sustainable Energy, Grids and Networks*, 6, 91–99.
- Mohammadiabadi, R., & Bilec, M. M. (2020). Application of machine learning for predicting building energy use at different temporal and spatial resolution under climate change in USA. *Buildings*, 10(8), 139.
- Molyneaux, L., Wagner, L., Froome, C., & Foster, J. (2012). Resilience and electricity systems: A comparative analysis. *Energy policy*, 47, 188–201.
- National Climate Change Committee. (2011). *Electrical consumption by appliance*. http://www.nccc.gov.sg/Households/es_guide.shtml.
- National Environment Agency. (2012). *NEA's Go green tips*. <https://www.cgs.gov.sg/what-we-do/programmes/eco-music-challenge/let's-go-green/nea's-go-green-tips>.
- Palme, M., Inostroza, L., Villacreses, G., Lobato-Cordero, A., & Carrasco, C. (2017). From urban climate to energy consumption: Enhancing building performance simulation by including the urban heat island effect. *Energy and Buildings*, 145, 107–120.
- Pokhrel, R., Ramrez-Beltran, N. D., & González, J. E. (2019). On the assessment of alternatives for building cooling load reductions for a tropical coastal city. *Energy and Buildings*, 182, 131–143.
- Quah, A. K., & Roth, M. (2012). Diurnal and weekly variation of anthropogenic heat emissions in a tropical city, Singapore. *Atmospheric Environment*, 46, 92–103.
- Robinson, C., Dilikina, B., Hubbs, J., Zhang, W., Guhathakurta, S., Brown, M. A., & Pendyala, R. M. (2017). Machine learning approaches for estimating commercial building energy consumption. *Applied Energy*, 208, 889–904.
- Santamouris, M., Papanikolaou, N., Livada, I., Koronakis, I., Georgakis, C., Argiriou, A., & Assimakopoulos, D. N. (2001). On the impact of urban climate on the energy consumption of buildings. *Solar energy*, 70(3), 201–216.
- Sharifi, A., & Yamagata, Y. (2016). Principles and criteria for assessing urban energy resilience: A literature review. *Renewable and Sustainable Energy Reviews*, 60, 1654–1677.
- Sheng, Z. (2021). Singapore country report. In *Energy outlook and energy saving potential in East Asia 2020* (p. 248).
- Tong, S., Wen, J., Wong, N. H., & Tan, E. (2021). Impact of façade design on indoor air temperatures and cooling loads in residential buildings in the tropical climate. *Energy and Buildings*, Article 110972.
- Tong, S., Wong, N. H., Tan, E., & Jusuf, S. K. (2019). Experimental study on the impact of facade design on indoor thermal environment in tropical residential buildings. *Building and Environment*, 166, Article 106418.
- Tso, G. K., & Yau, K. K. (2007). Predicting electricity energy consumption: A comparison of regression analysis, decision tree and neural networks. *Energy*, 32(9), 1761–1768.
- U.S. Department of Energy. (2016). *Auxiliary programs*. Energy Plus Version 8.5 Document.
- U.S. Department of Energy. (2021). *Tips and tricks for using EnergyPlus*. <https://energyplus.net/documentation>.
- Wang, H., Chen, W., & Shi, J. (2018). Low carbon transition of global building sector under 2-and 1.5-degree targets. *Applied Energy*, 222, 148–157.

- Watkins, R., Palmer, J., Kolokotroni, M., & Littlefair, P. (2002). The balance of the annual heating and cooling demand within the London urban heat island. *Building Services Engineering Research and Technology*, 23(4), 207–213.
- World Meteorological Organization. (2019). *WMO Confirms 2019 as second hottest year on record*. <https://public.wmo.int/en/media/press-release/wmo-confirms-2019-second-hottest-year-record>.
- Xie, X., Liu, C. H., Leung, D. Y. C., & Leung, M. K. H. (2006). Characteristics of air exchange in a street canyon with ground heating. *Atmospheric Environment*, 40(33), 6396–6409.
- Xie, X., Wang, S. S., & Tang, R. (2019). Probabilistic load forecasting for buildings considering weather forecasting uncertainty and uncertain peak load. *Applied Energy*, 237, 180–195.
- Yamaguchi, Y., Shimoda, Y., & Mizuno, M. (2007). Transition to a sustainable urban energy system from a long-term perspective: Case study in a Japanese business district. *Energy and Buildings*, 39(1), 1–12.
- Yang, X., Zhao, L., Bruse, M., & Meng, Q. (2012). An integrated simulation method for building energy performance assessment in urban environments. *Energy and Buildings*, 54, 243–251.
- Yang, Z., Ghahramani, A., & Becerik-Gerber, B. (2016). Building occupancy diversity and HVAC (heating, ventilation, and air conditioning) system energy efficiency. *Energy*, 109, 641–649.
- Yuan, C., Adelia, A. S., Mei, S., He, W., Li, X. X., & Norford, L. (2020). Mitigating intensity of urban heat island by better understanding on urban morphology and anthropogenic heat dispersion. *Building and Environment*, 176, Article 106876.
- Zhang, M. J., & Gao, Z. (2021). Effect of urban form on microclimate and energy loads: Case study of generic residential district prototypes in Nanjing, China. *Sustainable Cities and Society*, 70, Article 102930.
- Zhao, H. X., & Magoulès, F. (2012). A review on the prediction of building energy consumption. *Renewable and Sustainable Energy Reviews*, 16(6), 3586–3592.